IOP Publishing | Institute of Physics and Engineering in Medicine Physiological Measurement

Physiol. Meas. **35** (2014) 1665–1683 doi:10.1088/0967-3334/35/8/1665

A multi-step method with signal quality assessment and fine-tuning procedure to locate maternal and fetal QRS complexes from abdominal ECG recordings

Chengyu Liu[1,2], Peng Li[2], Costanzo Di Maria[3], Lina Zhao[2], Henggui Zhang[4] and Zhiqing Chen[5]

[1] School of Information Science and Engineering, Shandong University, Jinan, 250100, People's Republic of China
[2] School of Control Science and Engineering, Shandong University, Jinan, 250061, People's Republic of China
[3] Regional Medical Physics Department, Freeman Hospital, Newcastle upon Tyne NE7 7DN, UK
[4] Biological Physics Group, School of Physics and Astronomy, University of Manchester, Manchester M13 9PL, UK
[5] Second Affiliated Hospital, School of Medicine, Zhejiang University, Hangzhou, 310009, People's Republic of China

Email: bestlcy@sdu.edu.cn and chenzhiqing@medmail.com.cn

Received 12 February 2014, revised 11 June 2014
Accepted for publication 17 June 2014
Published 28 July 2014

Abstract

Non-invasive monitoring of fetal electrocardiogram (fECG) plays an important role in detecting and diagnosing fetal diseases. This study aimed to develop a multi-step method for locating both maternal and fetal QRS complexes from abdominal ECG (aECG) recordings. The proposed method included four major steps: abdominal ECG pre-processing, maternal QRS complex locating, maternal ECG cancellation and fetal QRS complex locating. Signal quality assessment (SQA) and fine-tuning for maternal ECG (FTM) were implemented in the first and third steps, respectively. The method was then evaluated using 75 non-invasive 4-channel aECG recordings provided by the PhysioNet/Computing in Cardiology Challenge 2013. The F_1 measure, which is a new index introduced by Behar *et al* (2013 *Proc. Comput. Cardiol.* **40** 297–300), was used to assess the locating accuracy. The other two indices, mean squared error of heart rate (MSE_HR) between the fetal HR signals estimated from the reference and our method (MSE_HR in bpm^2) and root mean squared difference between the corresponding fetal RR intervals (MSE_RR in ms) were also used to assess the locating accuracy. Overall, for the

maternal QRS complex, the F_1 measure was 98.4% from the method without the implementation of SQA, and it was improved to 99.8% with SQA. For the fetal QRS complex, the F_1 measure, MSE_HR and MSE_RR were 84.9%, 185.6 bpm^2 and 19.4 ms for the method without both SQA and FTM procedures. They were improved to 93.9%, 47.5 bpm^2 and 7.6 ms with both SQA and FTM procedures. These improvements were observed from each individual subject. It can be concluded that implementing both SQA and FTM procedures could achieve better performance for locating both maternal and fetal QRS complexes.

Keywords: fetal ECG, ECG QRS complex, signal quality assessment, fine-tuning for maternal ECG

(Some figures may appear in colour only in the online journal)

1. Introduction

Monitoring of fetal electrocardiography (fECG) during pregnancy and labor is very important and crucial for detecting fetal well-being and diagnosing the possible diseases. Abnormal fECG patterns (e.g., rapid acceleration-decelerations, reduced high-frequency variability, and pseudo-sinusoidal) can be signs of pathological conditions, such as fetal asphyxia, bradycardia and oxygen deficiency when some emergency intervention like cesarean delivery is needed. Therefore, fECG carries a significant importance for clinical perspectives (Clifford *et al* 2014, Hasan *et al* 2009, Kennedy 1998, Sameni and Clifford 2010).

fECG can be measured by applying an intra-uterine electrode on the fetal scalp or from skin electrodes attached to the mother's abdomen (Lai and Shynk 2002, Clifford *et al* 2011). fECG from the intra-uterine scalp electrode is much clearer than using non-invasive skin electrodes, but it is invasive with high risks of infection during internal monitoring, and is not suitable for long term monitoring or during labor after the breaking of the amniotic fluid (Clifford *et al* 2014, Martens *et al* 2007, Sameni *et al* 2008). In contrast, abdominal fECG is non-invasive and offers the possibility for long-term monitoring of the basal fetal heart rate (fHR), fHR variability and the process of different pathological conditions (Hasan *et al* 2009, Ingemarsson 2009).

However, fECG recorded non-invasively from the mother's abdomen is inevitably contaminated by a variety of other physiological signals and noises. Among them, maternal ECG (mECG) is the predominant interference source with much larger amplitude than fECG. Moreover, the frequency spectrum of mECG partially overlaps that of fECG and therefore filtering alone is not sufficient to extract fECG (Camps-Valls *et al* 2004, Hasan *et al* 2009). Other noises include baseline drift, 50 or 60 Hz power-line interference, respiration interference, maternal electromyogram (EMG), electrode contact noise and motion artefacts (Martens *et al* 2007, Sameni and Clifford 2010, Clifford *et al* 2011). Until now, despite significant advances in signal processing techniques for adult clinical ECG, few significant advances have been made in the analysis of non-invasive fECG (Behar *et al* 2013). It is mainly because of the poor signal-to-noise ratio (SNR) of fECG caused by the different interference signals and noises mentioned above. The other reasons include the temporal and spectral overlap between fECG and the noises, as well as the morphological similarity between fetal and maternal QRS complexes (Sameni and Clifford 2010, Andreotti *et al* 2013, Behar *et al* 2013). Therefore, it is still a clinical challenge to effectively extract fECG and its characteristics.

Numerous attempts have been made to retrieve the real fECG from the abdominal recordings. It has been reviewed (Clifford *et al* 2014, Sameni *et al* 2008) that the main methods for fECG extraction include adaptive filtering, linear decomposition and non-linear decomposition. Adaptive filtering methods train an adaptive or matched filter to remove the mECG (Outram *et al* 1995), or to directly extract the fECG (Park *et al* 1992). The drawback of adaptive filtering methods is that they require a reference mECG signal or several linearly independent channels to roughly reconstruct the morphological shape of the mECG to achieve mECG removal (Sameni and Clifford 2010), which is inconvenient to obtain, and the morphology of mECG is highly dependent on the electrode locations. As a variant of adaptive filters, the Kalman filter has recently been shown as a promising method for mECG cancellation and fECG extraction (Sameni *et al* 2008). Linear decomposition methods decompose the abdominal ECG recordings into different components (mECG, fECG and noises) by using fixed or data-driven basis functions. Wavelet decomposition (Khamene and Negahdaripour 2000), matching pursuits (Akay and Mulder 1996), blind or semiblind source separation (De Lathauwer *et al* 2000), singular value decomposition (SVD) (Kanjilal *et al* 1997), principal component analysis (PCA) (Kanjilal *et al* 1997) and independent component analysis (ICA) (Najafabadi *et al* 2006) are the most commonly used linear decomposition methods for fECG extraction and denoising. However, one of the limitations of linear decomposition methods is that mECG, fECG and noises are assumed to be a linear and stationary mixture, whereas this assumption is usually not a good approximation due to the respiration interference, electrode contact noise and motion artefacts. Another limitation is that linear decomposition methods could be regarded as spatial filters rather than temporal filters. So they have not been fully customized to the periodic structures of both mECG and fECG (Sameni and Clifford 2010). For the non-linear decomposition methods, non-linear projection (Richter *et al* 1998) and deflation method of subspace decomposition are usually used for mECG cancellation and fECG enhancement. These non-linear methods have been shown to be very promising and are even competent to extract fECG from low SNR abdominal recordings. Nevertheless, high computational complexity in non-linear methods could not be disregarded, which makes real-time processing difficult. To better understand the state-of-the-art of the relevant research, the review article from Sameni and Clifford (2010) is highly recommended.

The PhysioNet/Computing in Cardiology Challenge 2013 called for the development of different methods to extract fECG information from 4-channel maternal abdominal ECG (aECG). It attracted a total of 53 teams to attend (Clifford *et al* 2014, Silva *et al* 2013); most teams first removed the maternal QRS from the original aECG and then extracted the fetal QRS from the residual signals. Among them, Behar *et al* employed a fusion method of several different mECG extraction algorithms and obtained the best Challenge scores on the validation set (Behar *et al* 2013). Other techniques with high Challenge scores included an extended Kalmam smoother and template adaption (Andreotti *et al* 2013), subspace decomposition and reconstruction (Lipponen and Tarvainen 2013), RS slope detection (Podziemski and Gierałtowski 2013), expectation weighting method (Di Marco *et al* 2013), adaptive linear filter (Rodrigues 2013), ICA (Varanini *et al* 2013), PCA (Di Maria *et al* 2013) and signal quality assessment with adaptive template matching method (Liu and Li 2013).

The aim of this study was to improve our method for the PhysioNet Challenge 2013 (Liu and Li 2013). A multi-step method was developed and evaluated for locating both maternal and fetal QRS complexes from 4-channel aECG recordings. Two distinctive sub-steps in the improved method were implemented: (1) ECG signal quality assessment (SQA) based on sample entropy before maternal QRS detection, and (2) fine-tuning for mECG (FTM). The SQA implementation was based on the fact of that the signal quality of aECG recordings varies and the unexpected noises seriously affect the extraction of fECG information. The use of FTM was

to weaken the impulse interferences appearing at the location of maternal QRS complex during mECG cancellation. Our improved method was finally evaluated by comparing the results between both without and with SQA and FTM procedures.

2. Methods

2.1. Dataset

The PhysioNet/Computing in Cardiology Challenge 2013 provided a collection of one-minute non-invasive aECG recordings. Each recording included four channels and they were sampled at 1000 Hz with 16-bit resolution. Seventy-five aECG recordings (a01 ~ a75) in training set A with the reference annotations for each fetal QRS complex were analyzed in this study. The reference annotations were produced by experts with reference to a direct fECG signal, acquired from a fetal scalp electrode. More detailed information can be found in Clifford *et al* (2014) and Silva *et al* (2013).

2.2. Method description

Figure 1 shows the block diagram of the multi-step method for locating both maternal and fetal QRS complexes. This method consisted of four major steps. Step 1: abdominal ECG pre-processing; step 2: maternal QRS complex location; step 3: maternal ECG cancellation and step 4: fetal QRS complex location. The details of each step are described in the following. Two distinctive sub-steps (SQA and FTM) were implemented in steps 1 and 3. They will be specially emphasized.

2.3. Step 1: abdominal ECG pre-processing

2.3.1. A1i filtering. Firstly, common power-line interference was removed using a notch filter (Hamilton 1996). The baseline wander was then removed using a low-pass filter based on the wavelet transform method (Quan *et al* 1999). The baseline wander below 1 Hz was removed for the following steps analysis except for the SQA procedure. For SQA, the baseline wander below 8 Hz was removed. The filtering operations also included high frequency noise removal by wavelet soft-threshold de-noising after sub-step A3.

2.3.2. A2: signal quality assessment. The quality assessment for physiological signals plays an important role in the accurate characteristic estimation and is crucial for clinical judgment (Li *et al* 2008). Entropy has been proven to be a useful tool for noise identification from ECG recordings (Liu *et al* 2011a). In this study, the filtered aECG signal was analyzed using the sample entropy (SampEn) method to determine if it included too many noise components. Each channel of the aECG signal was first divided into six non-overlapping episodes (10 s each). Then each episode was re-sampled to have a constant length of 500 with its SampEn value calculated. The mean of the six SampEn values for each channel of aECG was then obtained. Signal quality was assessed by comparing the mean SampEn value from each channel with a constant threshold value, which was empirically set at 1.5 for aECG recordings from the PhysioNet/Computing in Cardiology Challenge 2013. The channels with the mean SampEn value larger than 1.5 were regarded as poor quality and were excluded from the following analysis in steps 2, 3 and 4. However, if less than two channels of good quality returned, the two channels with the smallest and penultimate SampEn values were retained for further analysis. Figure 2(*a*) shows an example of signal quality assessment for a 10 s signal

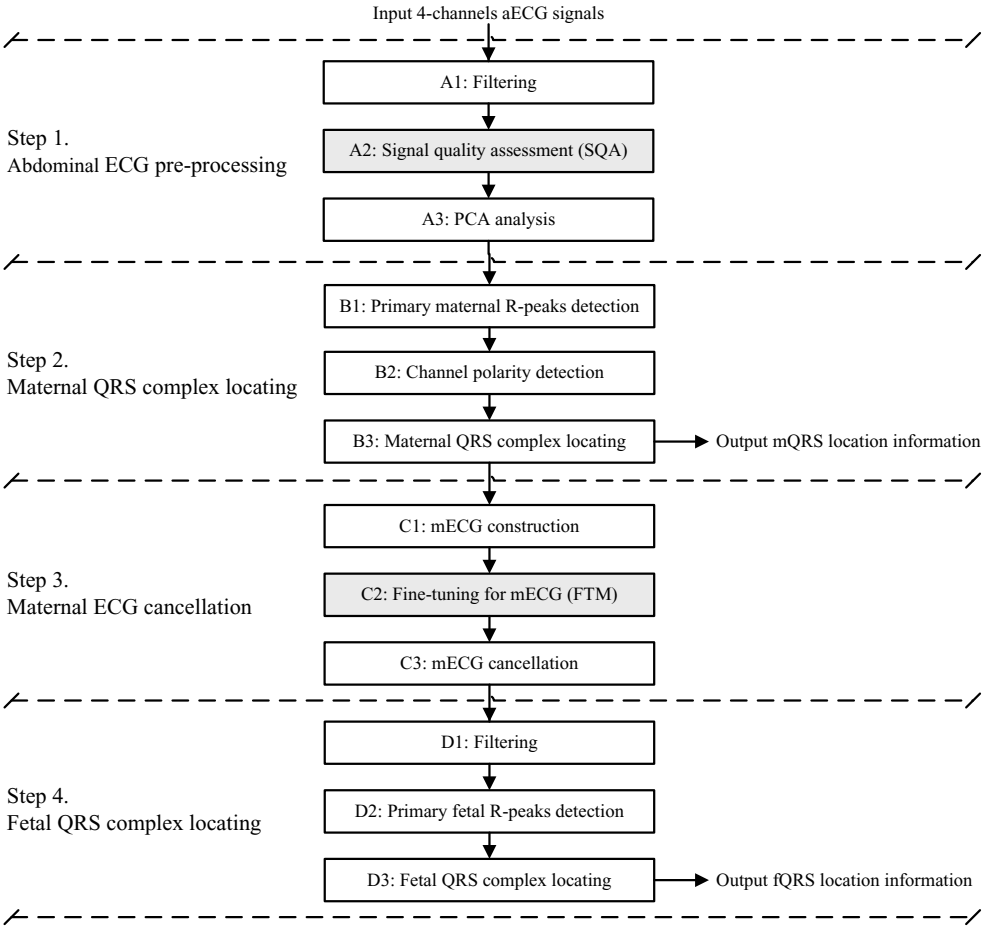

Figure 1. Block diagram of the proposed multi-step method. Four steps are progressively connected for location of both maternal and fetal QRS complexes. In each step, there are three sub-steps. A2 signal quality assessment (SQA) and C2 fine-tuning for mECG (FTM) are two distinctive sub-steps in this study.

episode from the recording a40, in which channels 1 and 3 were excluded since their SampEn values were larger than the threshold 1.5, while channels 2 and 4 were kept for the following analysis. It also can be seen from figure 2(*a*) that the threshold value of 1.5 is relatively rigid and only very poor signal quality channels were excluded. The detailed calculation process of SampEn and the experimental validation of its efficiency for signal quality assessment of filtered aECG signals are summarized in the appendix.

2.3.3. A3: PCA analysis. After signal quality assessment, the aECG channels with good signal quality after the notch filter and 0 ~ 1 Hz baseline wander removal were analyzed using the PCA method to obtain the first principal component of aECG recordings (Jolliffe 2005). Figures 2(*b*) and (*c*), respectively, show the first principal components from all four aECG channels (without the SQA procedure) and from the two selected channels (with the SQA procedure).

The signal quality of the first principal component was again assessed using the SampEn method. Based on the SampEn results of the four filtered aECG channels and their first

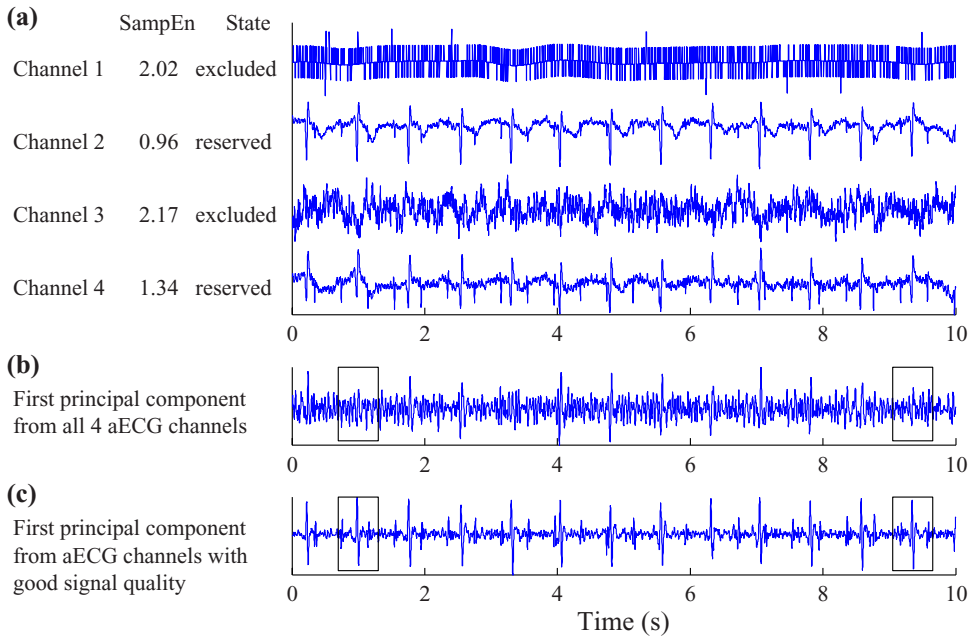

Figure 2. (*a*) An example of signal quality assessment for a 10 s signal episode from recording a40. The principal components of this aECG recording were extracted and compared using all four aECG channels (*b*) and channels with good signal quality (*c*). It is clearly shown that with the signal quality assessment, the principal component has more obvious characteristics of the maternal QRS complex, from which the maternal QRS complex can be easily located. The comparisons of the maternal QRS proportion between all four aECG channels (*b*) and from two selected channels (*c*) have been highlighted in the two rectangular ranges of these 10 s signals.

principal components, an optimal reference signal was determined. If the SampEn of the first principal component was lower than 1.5 times the smallest SampEn from four aECG channels, the optimal reference signal was the first principal component. Otherwise, the optimal reference signal was the aECG channel with the smallest SampEn value. The optimal reference signal, as well as the filtered aECG channels with good signal quality, was then input into step 2.

2.4. Step 2: maternal QRS complex location

2.4.1. B1: primary maternal R-peak detection. The maternal R-peaks were primarily detected from the selected optimal reference signal using an adaptive QRS detector proposed by Pan and Tompkins (1985). The constant period for the maternal QRS complex was set as 220 ms. The false positive and false negative of R-peak detection were corrected by Liu's method (Liu *et al* 2012). The detected maternal R-peaks were regarded as the reference maternal QRS complexes.

2.4.2. B2: channel polarity detection. After the primary identification of the maternal R-peaks, the R-peak polarities in channels with good signal quality were determined. For each channel, the QRS complex segments with 0.3 s length were extracted. Two parameters $N_{po} = 0$ and $N_{ne} = 0$ were initiated to respectively denote the numbers of positive and negative

polarities of QRS complex. For each QRS complex segment, if the difference between the maximum and mean value was larger than that between the mean value and minimum, N_{po} was added by 1. If not, N_{ne} was added by 1. If the final N_{po} was larger than N_{ne}, the polarity of the analyzed channel was labeled as 'positive', otherwise 'negative'.

2.4.3. B3: maternal QRS complex location. For each channel of the aECG signal with good quality, the maternal QRS complex was located as follows: if the channel polarity was 'positive', the maxima in a constant time window of 150 ms centered with the reference maternal QRS locations were determined as the actual locations of maternal R-peaks. If the channel polarity was 'negative', the minima in a constant time window 100 ms centered with the maternal reference QRS locations were determined as the actual locations of maternal R-peaks. The maternal RR interval sequences were obtained by differencing the consecutive R-peaks in the channels with good signal quality. The channel with the smallest SD was selected as the final maternal RR interval sequence and their corresponding maternal R-peaks were determined as the final maternal QRS complex location.

2.5. Step 3: maternal ECG cancellation

2.5.1. C1: mECG construction. For each aECG channel with good signal quality, the mECG template was constructed using the coherent averaging method. All the episodes with normal amplitudes and intervals from two consecutive R-peaks were extracted and stretched to the constant 1000 points length to facilitate the average processing. The mECG template was the average of these episodes after stretching. Next, the constructed mECG signals were obtained by first re-stretching the mECG template to the actual length of each period and then joining them beat-by-beat.

2.5.2. C2: fine-tuning for mECG. After mECG construction, a fine-tuning procedure was used to achieve the optimal matching between the filtered aECG and reconstructed mECG signals. The implementation process is shown in figure 3. Both the reconstructed mECG signal and the filtered aECG signal were first up-sampled using 10 times the original sample rate, i.e., 10 KHz. Then the matching operation was performed and correlation degree was calculated for each QRS complex segment (0.3 s) between the reconstructed mECG signal and the filtered aECG signal. The matching operation is just shift the signal left or right to achieve the maximum correlation degree to make sure that a more identifiable fECG signal could be obtained after subtracting the reconstructed mECG from the filtered aECG. Figure 4 shows an example of the performance of the FTM procedure for one QRS complex segment from recording a37, and the corresponding optimal fECG signals with and without the FTM procedure are also given. For information on the optimal fECG signal, please see section 2.6.3.

2.5.3. C3: mECG removal. In this sub-step, the fECG signals were obtained by subtracting the reconstructed mECG after FTM procedure from the filtered aECG channels. The FTM procedure produces the best maternal signal matching between the reconstructed mECG and the filtered aECG. So the acquired fetal QRS complex is obvious even when the fetal QRS complex superimposed on the maternal one (see figure 4(*c*) at time of 4 s).

2.6. Step 4: fetal QRS complex location

2.6.1. D1: filtering. In this sub-step, the baseline wander (0 ~ 2 Hz) of fECG signals was removed using the wavelet transmit method (Quan *et al* 1999).

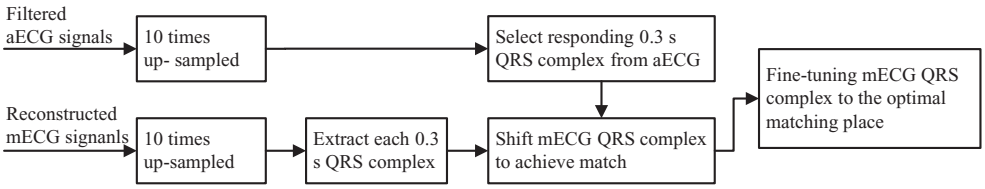

Figure 3. Flow chart of the fine-tuning for the mECG procedure.

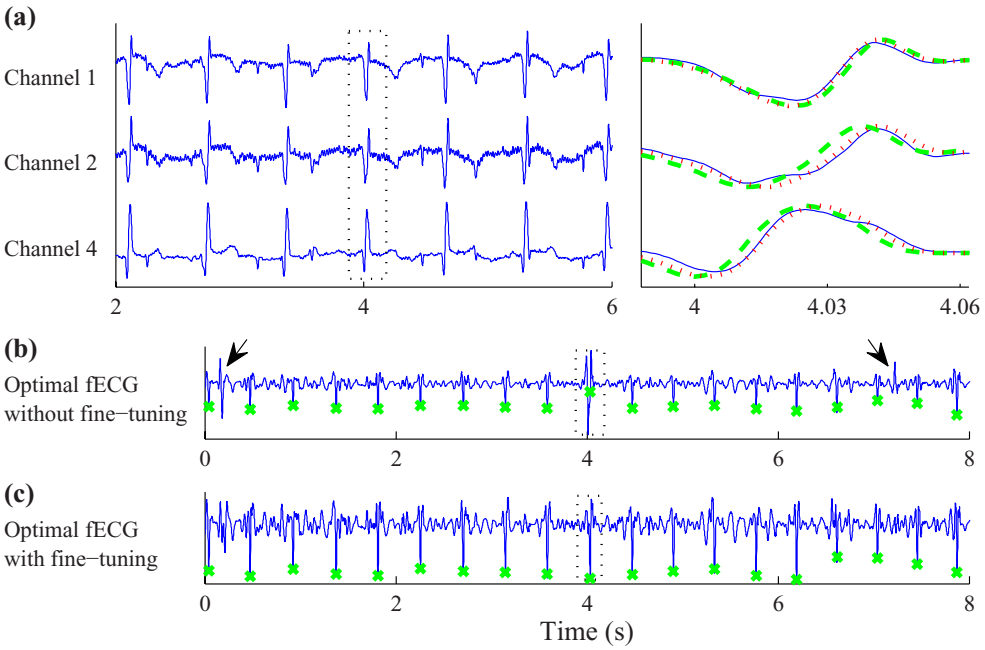

Figure 4. (*a*) An example of the fine-tuning procedure for a signal episode from recording a37 and its corresponding optimal fECG signals without (*b*) and with (*c*) this fine-tuning procedure. The *x*-axis in each sub-figure shows the time (s). In the left panel of sub-figure (*a*), channels with good quality of aECG are given. In the right panel of sub-figure (*a*), a maternal QRS complex (blue solid line) from a filtered aECG is given with its corresponding template QRS complexes from without (green dashed line) and with (red dotted line) the fine-tuning procedure. In sub-figure (*b*), it is clearly shown that the optimal fECG signal without the fine-tuning procedure has many unexpected impulses when maternal QRS complexes happen (the dashed box near the time of 4 s, as well as two places indicated by the arrows). These unexpected impulses disappear after using the fine-tuning procedure in (*c*). The green cross ' × ' shows the reference annotations for fetal QRS complex location.

2.6.2. D2: primary fetal R-peak detection. Firstly, the first principal component of the fECG signals was extracted by the PCA method (Jolliffe 2005). The fetal R-peaks in each channel of fECG signals and their first principal component were then detected by Pan and Tompkins' method, which employed a constant time length 150 ms for the fetal QRS complex (Pan and Tompkins 1985).

2.6.3. D3: fetal QRS complex location. The fetal RR interval sequences were obtained by differencing the consecutive R-peaks from each channel of fECG signals and their first principal component. The fetal RR interval sequence with the smallest SD was selected as the final fetal RR interval sequence, and its corresponding signal (one fECG channel or the first principal component) was used as the optimal fECG signal. These fetal R-peaks in the optimal fECG signal were selected as the final fetal QRS complex locations that were smoothed by Liu's method to remove the false positive and false negative R-peaks (Liu *et al* 2012).

2.7. Evaluation scheme

The evaluation scheme for the accuracy of locating both maternal and fetal QRS complexes is summarized in figure 5. For the maternal QRS complex, our improved method was compared with or without SQA. For the fetal QRS complex, it was compared without SQA or FTM or both.

The F_1 measure was used as the evaluation index for locating both maternal and fetal QRS complexes (Behar *et al* 2013), which is defined as follows:

$$F_1 = \frac{2\times \mathrm{TP}}{2\times \mathrm{TP} + \mathrm{FP} + \mathrm{FN}} \tag{1}$$

where TP is the number of QRS complexes truly detected, FP is the number of false positive (extra falsely detected QRS complex) and FN is the number of false negative (missed detected QRS complex).

The actual maternal QRS complex locations were acquired beat-by-beat by a trained ECG technician for all 75 aECG recordings. The actual fetal QRS complex locations were from the reference annotations provided by the PhysioNet/Computing in Cardiology Challenge 2013. For each actual QRS complex, the detected QRS complex was considered to be matched if they were within 100 ms. If there were not matched, FN was added by 1; FP was the number of the detected QRS complexes appearing beyond 100 ms of the actual QRS complexes. FP and FN played a symmetric role in penalizing the F_1 measure. To calculate the F_1 measure, the first and last 1 s segments of each recording were discarded.

Another two indices, MSE_HR in bpm^2: the mean squared error between the fHR signals estimated from the reference and test annotations and MSE_RR in ms: the root mean squared difference between corresponding RR intervals, were also used to evaluate the accuracy of locating fetal QRS complexes. To calculate MSE_HR, the reference fetal QRS annotation sequence was formed 17 half-overlapping 6 s segments, (from 3–9 s, 6–12 s,…, 51–57 s). For the ith 6 s segment, the current reference fetal HR $\mathrm{fHR}_{\mathrm{ref}}(i)$ and test fetal HR $\mathrm{fHR}_{\mathrm{test}}(i)$ were calculated. MSE_HR for the current aECG recording was calculated as $\mathrm{MSE\_HR}=\frac{1}{K1}\sum_{i=1}^{K1}(\mathrm{fHR}_{\mathrm{ref}}(i)-\mathrm{f}H\mathrm{R}_{\mathrm{test}}(i))^2$, where $K1$ is the number of segments with reference fHR more than 60 bpm and the segments with reference fHR no more than 60 bpm have been excluded for the calculation. To calculate MSE_RR, the reference fetal RR intervals with values no less than 1000 ms also be excluded. The MSE_RR was calculated as $\mathrm{MSE\_RR}=\frac{1}{K2}\sum_{i=1}^{K2}\min(\min(|\mathrm{fRR}_{\mathrm{ref}}(i)-\mathrm{fRR}_{\mathrm{test}}|),100)$, where $K2$ is the number of reference fetal RR intervals with values less than 1000 ms and $\mathrm{fRR}_{\mathrm{test}}$ is the test fetal RR sequence.

For each aECG recording, the above three indices were calculated with their average values obtained from all 75 recordings.

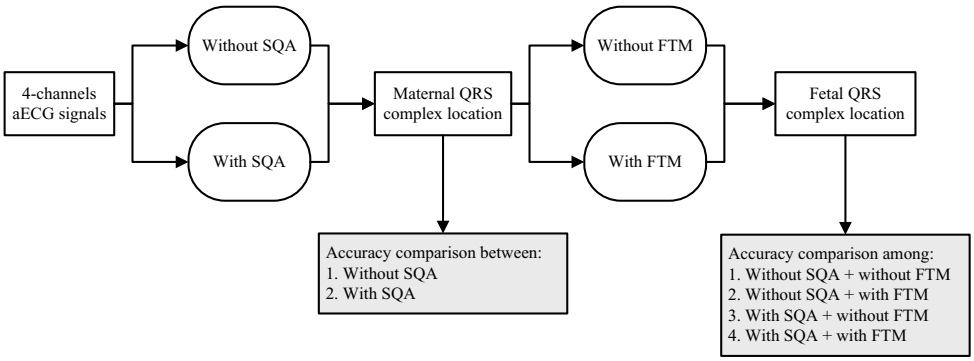

Figure 5. The evaluation scheme for the accuracy of locating both maternal and fetal QRS complexes.

3. Results

3.1. Examples of locating the QRS complex using the proposed multi-step method

Figure 6 gives an example of locating the QRS complex (10 s length) using the proposed multi-step method from aECG recording a05. In sub-figure (*a*), aECG channels 1, 3 and 4 were assessed as the good signals by the SampEn method. The optimal reference signal of this aECG recording is shown at the bottom of sub-figure (*a*) with the detected R-peaks (black circle '●'). With the location of these R-peaks and the results from the channel polarity detection, R-peaks in each aECG channel were determined and also marked with a black circle '●'. The reconstructed mECG signals after the fine-tuning procedure are shown in sub-figure (*b*). They are quite clear since the coherent averaging method decreases the noise level, allowing the easy and accurate extraction of fECG. Sub-figure (*c*) shows the fECG signals by subtracting the reconstructed mECG from the filtered aECG signals. The optimal fECG signal is also shown at the bottom of this sub-figure. The black square '■' shows the detected R-peaks in each fECG channel; the red circle '○' shows the final location of the fetal QRS complex and the green cross ' × ' gives the reference location of the fetal QRS complex. It is clearly shown that the estimated locations of the fetal QRS complex are almost same as those from the reference.

3.2. Intermediate results after signal quality assessment and fine-tuning for mECG

As shown in figure 7(*a*), from all 75 aECG recordings, with SQA, 30 aECG recordings were detected with at least one poor signal quality channel (total 41 channels). These channels were excluded from further analysis. Figure 7(*b*) shows the shift times after the FTM procedure. The mean and SD of shift time from all 75 aECG recordings were -0.04 ms (shift left) and 0.05 ms.

3.3. Evaluation results of the proposed multi-step method

As shown in table 1, the number TP of total actual maternal and fetal QRS complexes was 6431 and 10169. For the maternal QRS complex, the method without SQA truly detected 6354 (TP) QRS complexes, falsely detected 126 (FP) extra QRS complexes and missed 77 (FN)

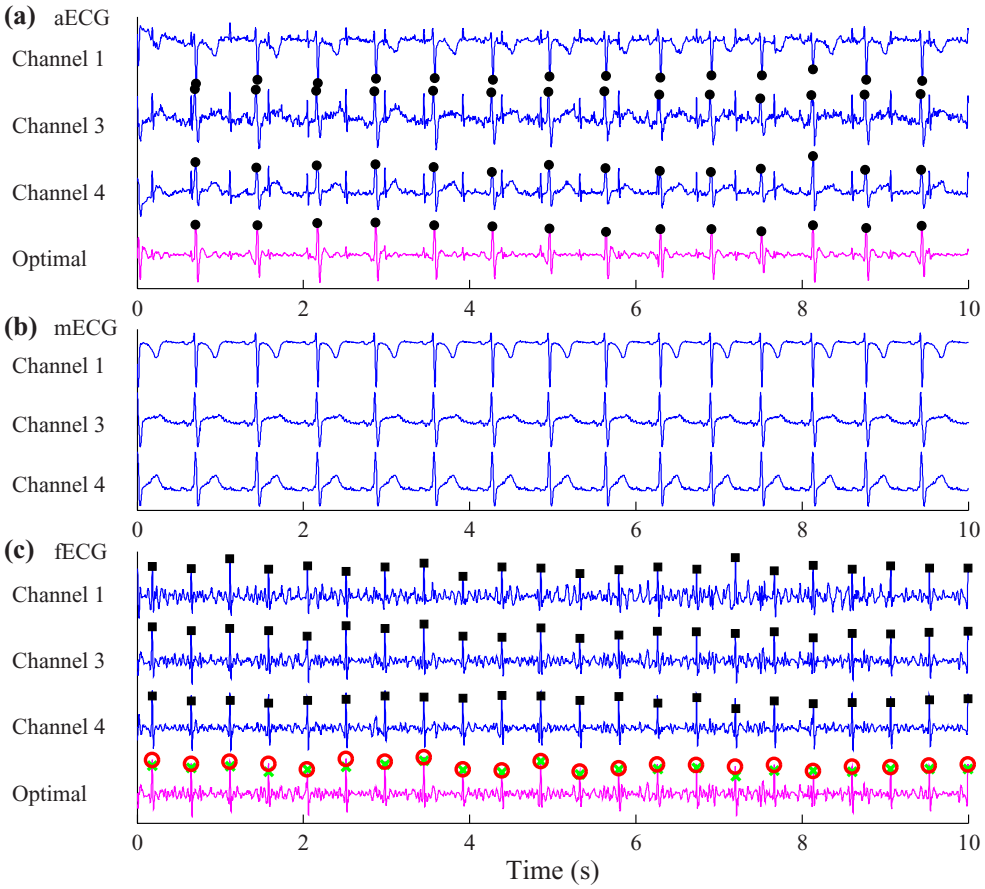

Figure 6. An example of locating QRS complexes using the proposed multi-step method from aECG recording a05. (*a*) aECG channels with good signal quality and the optimal aECG reference signal, (*b*) reconstructed mECG signals, (*c*) fECG signals and the optimal fECG. The detected maternal R-peaks (black circle '●') and fetal R-peaks (black square '■'), as well as the locations of fetal QRS complex from the estimated (red circle '○') and reference (green cross ' × '), are also given.

actual QRS complexes, which produced an F_1 measure of 98.4%. By contrast, the method with SQA truly detected 6413 (TP) QRS complexes, only falsely detected 11 (FP) extra QRS complexes and missed 18 (FN) actual QRS complexes, which made an F_1 measure of 99.8%.

For the fetal QRS complex, F_1 measure, MSE_HR and MSE_RR were 84.9%, 185.6 bpm^2 and 19.4 ms from the algorithm without the implementation of both SQA and FTM. With both SQA and FTM, they were improved to 93.9%, 47.5 bpm^2 and 7.6 ms. This improvement was observed in each individual recording, as shown in figure 8. Therefore, implementing both the SQA and FTM achieved the best performance for locating the fetal QRS complex.

4. Discussion

A multi-step method has been developed to locate both the maternal and fetal QRS complexes. Its accuracy has been evaluated using 75 non-invasive 4-channel abdominal ECG recordings

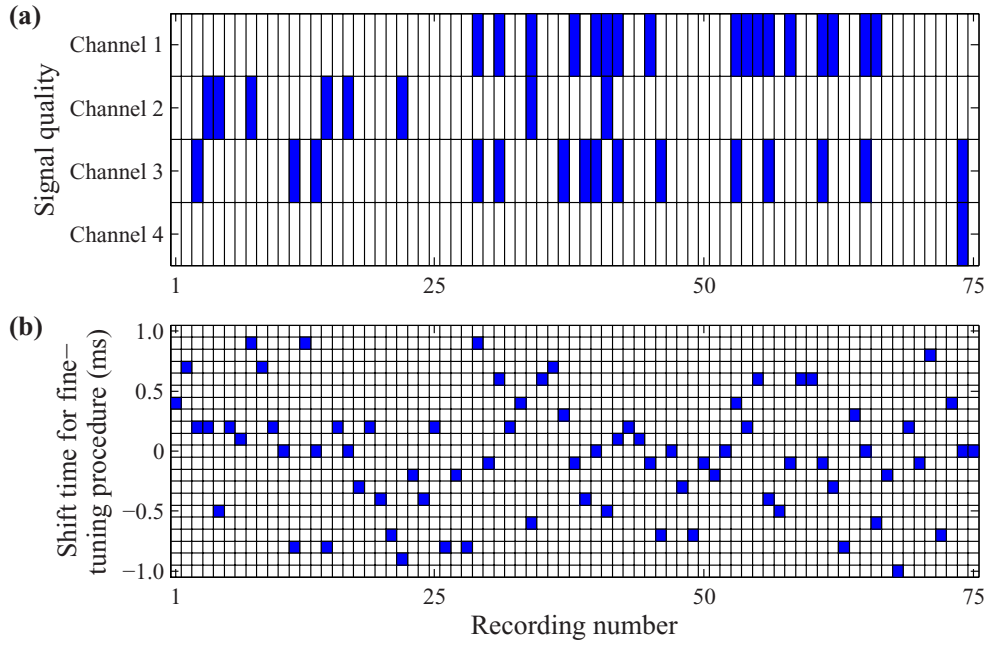

Figure 7. (*a*) Results of signal quality assessment using the SampEn measure. Blue label '■' means that the signal in the current aECG channel is poor and this channel is excluded. (*b*) Results of shift time from the fine-tuning for mECG procedure for each recording. The shift time is labeled as '■' and negative means shift left while positive means shift right. For each recording, the shift time is the mean value of shift times from all the mECG QRS complexes in that recording.

Table 1. Evaluation results of the proposed multi-step method for locating both maternal and fetal QRS complexes from all 75 aECG recordings.

Method	TP	FP	FN	F_1 (%)	MSE_HR (bpm^2)	MSE_RR (ms)
Locating maternal QRS complex						
Without SQA	6354	126	77	98.4	—	—
With SQA	6413	11	18	**99.8**	—	—
Locating fetal QRS complex						
Without SQA + Without FTM	8496	1341	1673	84.9	185.6	19.4
Without SQA + With FTM	9037	867	1132	90.0	98.9	10.7
With SQA + Without FTM	9265	1088	904	90.3	91.8	9.9
With SQA + With FTM	9573	639	596	**93.9**	**47.5**	**7.6**

Note: SQA, signal quality assessment; FTM, fine-tuning for mECG.

from the PhysioNet/Computing in Cardiology Challenge 2013 (Clifford *et al* 2014, Silva *et al* 2013). Compared with the conventional multi-step method, two distinctive sub-steps (SQA based on SampEn and FTM) were implemented. The results demonstrated the improvement of locating QRS complexes by implementing these two distinctive procedures.

In this study, SampEn was used to assess the signal quality. The most important role of the SQA procedure was to exclude the channels with strong noises because the channels with strong noises would contaminate the PCA results. It is noted that when using SampEn based SQA for the real aECG signals, the threshold value was set to be 1.5, which was really rigid

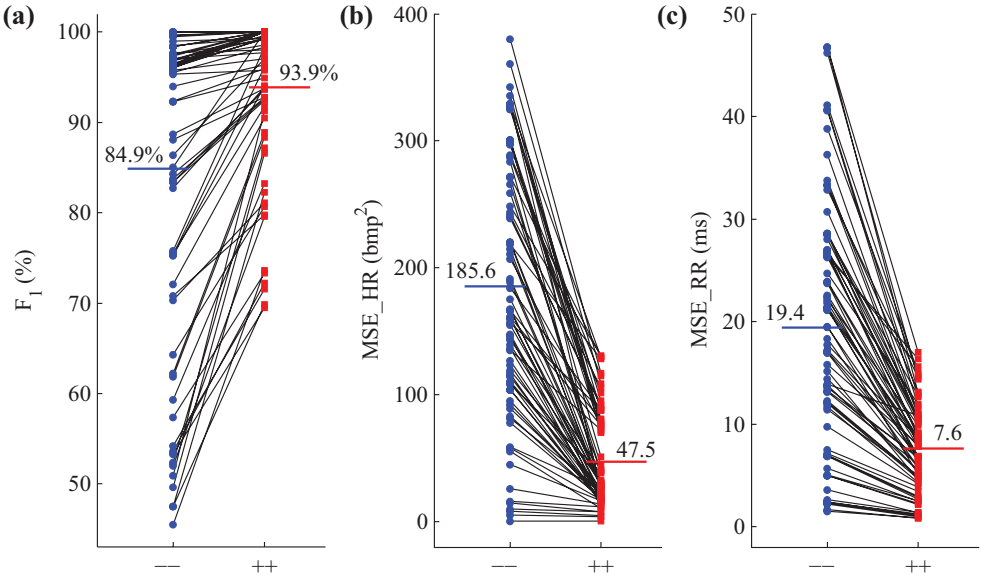

Figure 8. Changes of the F_1 measure (*a*), MSE_HR (*b*) and MSE_RR (*c*) for locating the fetal QRS complex with and without the implementation of both SQA and FTM procedures for each individual of the 75 aECG recordings. Their mean values are also given. − − : without the implementation of both SQA and FTM procedures. ++: with the implementation of both SQA and FTM procedures.

Table 2. Performances for locating both maternal and fetal QRS complexes from all 75 aECG recordings when using different SampEn threshold values.

	SampEn threshold values				
Indices	1.0	1.25	1.5	1.75	2.0
Locating maternal QRS complex with SQA					
F_1 (%)	98.6	99.4	**99.8**	99.7	98.9
Locating fetal QRS complex with SQA and FTM					
F_1 (%)	91.1	93.3	**93.9**	93.4	92.0
MSE_HR (bpm^2)	79.6	56.9	**47.5**	55.3	68.4
MSE_RR (ms)	9.2	8.0	**7.6**	7.9	8.5

for excluding the channels with poor signal quality. It can be seen from figure 2(*a*) that only very poor signal quality channels were excluded. Figures 2(*b*) and (*c*) clearly showed that with the SQA procedure, the maternal components of the PCA result are more obvious, which makes for easier detection of maternal QRS complexes. It can also be seen from the simulated results in Figure A1 that for $r = 0.20$, simulated aECG with SampEn higher than 1.5 are fully submerged with strong noises and very little maternal and fetal information could be seen. For validating the threshold 1.5 of SampEn, the performances for locating both maternal and fetal QRS complexes from all 75 aECG recordings were analyzed using different threshold values from 1.0 to 2.0 with a step of 0.25, i.e., 1.0, 1.25, 1.5, 1.75 and 2.0. The results are summarized in table 2. When using threshold 1.5, the best performance has been achieved. These additional results also prove the selection of threshold 1.5 for SampEn.

It should be also noted that the SampEn values rely on the parameter setting (mainly the threshold r, as well as the embedded dimension m and the data length N) (Liu *et al* 2011b).

Table 3. Evaluation results of the proposed multi-step method for locating both maternal and fetal QRS complexes for selected 67 aECG recordings.

Method	TP	FP	FN	F_1 (%)	MSE_HR (bpm^2)	MSE_RR (ms)
Locating maternal QRS complex						
Without SQA	5846	67	41	99.1	—	—
With SQA	5887	0	0	**100**	—	—
Locating fetal QRS complex						
Without SQA + Without FTM	8066	1159	1374	86.4	143.5	15.7
Without SQA + With FTM	8409	722	1031	90.6	85.1	9.3
With SQA + Without FTM	8683	819	757	91.7	76.8	8.8
With SQA + With FTM	8967	595	473	**94.4**	**36.7**	**6.9**

Note: the aECG recordings a29, a33, a38, a47, a52, a54, a71 and a74 are excluded due to the inaccurate reference annotations of fetal QRS complex or unclear maternal QRS complex. SQA, signal quality assessment; FTM, fine-tuning for mECG.

Nevertheless, a promising result has been achieved by including the entropy-based signal quality assessment. Recently, some researchers improved the entropy methods based on the combination of fuzzy theory and entropy, resulting in better algorithm stability and consistency than those of conventional entropy measures (approximate Entropy (ApEn) and SampEn) (Liu *et al* 2013). These improved entropy methods provide new sights for the signal quality assessment and it is worth assessing their performance for locating the fetal QRS complex in future.

Fine-tuning for the mECG procedure could enhance the matching degree between the original aECG and reconstructed mECG signals, and hence produce a more identifiable fECG signals. The non-optimal matching between the original aECG and reconstructed mECG signals is mainly due to the inadequate sampling rate (1 KHz). It has been shown that shifting the reconstructed mECG to the left or right one sample point (1 ms) could not achieve the optimal matching, and it could be obtained by shifting the reconstructed mECG a decimal value (between 0 and 1 ms). So both aECG and mECG signals were up-sampled 10 times to achieve the optimal matching. Another reason for the non-optimal matching is that the original aECG sometimes has two maximum or minimum values when an R-peak occurs. In this situation, without the fine-tuning procedure, the impulse interferences at the maternal QRS complexes usually appear, which eventually affect the detection of fetal R-peaks.

Moreover, because the scoring indices of MSE_HR and MSE_RR are based on a root mean square measure and are very sensitive to the false detection beyond the 100 ms range of the actual QRS complex, it is better to be slightly off the fetal QRS complex location all the time than have a few bad outliers (Behar *et al* 2013). So we also included a new F_1 measure to re-evaluate the location accuracy. The F_1 measure combines the algorithm sensitivity and specificity in one formula and could make for a more objective assessment of different methods.

As suggested in Behar *et al* (2013), seven aECG recordings (a33, a38, a47, a52, a54, a71 and a74) had inaccurate reference annotations of the fetal QRS complex identified by visual inspection. In addition, the maternal QRS complex in an aECG recording (a29) could not be clearly identified by visual inspection. So we excluded these eight recordings and re-evaluated the performance of our proposed method. The number TP of total actual maternal and fetal QRS complexes changed to 5887 and 9440, respectively. Table 3 shows the evaluation results for the remaining 67 aECG recordings. Relatively better results have been acquired. For the maternal QRS complex location, the method without SQA falsely detected 67 (FP) extra QRS complexes, missed 41 (FN) actual QRS complexes and gave an F_1 measure of 99.1%. The method with SQA had an F_1 measure of 100%. For the fetal QRS complex location, the best performances

of F_1, MSE_HR and MSE_RR from using the combination of SQA and FTM increased 0.5%, 10.8 bpm^2 and 0.7 ms, respectively, compared with those when using all 75 recordings. In addition, to validate the efficiency, the proposed method could also be tested on testing set B (100 aECG recordings) from the PhysioNet/Computing in Cardiology Challenge 2013 with the results of MSE_HR 264.87 bpm^2 and MSE_RR 9.04 ms using the online scoring system.

In conclusion, we have proposed an improved multi-step method with the SQA and TFM procedures to locate both maternal and fetal QRS complexes. Its good performance has been confirmed with very high locating accuracy, even for recordings with 1 or 2 channels of noisy aECG signals.

Acknowledgements

This work was supported by the National Natural Science Foundation of China under Grant 61201049, the Excellent Young Scientist Awarded Foundation of Shandong Province in China under Grant BS2013DX029, Public Welfare Technology Project of Science Technology Department of Zhejiang Province under Grant 2012C23068, the China Postdoctoral Science Foundation under Grant 2013M530323, the Postdoctoral Innovation Foundation of Shandong Province in China under Grant 201303102 and Zhejiang Province Medical Platform Program under Grant 2013RCB008.

Appendix. Signal quality assessment of filtered aECG based on sample entropy

Sample entropy (SampEn) is a good measure to quantify signal irregularity. A larger SampEn corresponds with an increase in Gaussian noise and other noise. The calculation process of SampEn is summarized as follows (Richman and Moorman 2000): for the re-sampled aECG episode sequence $u(i)$, $1 \le i \le N$ (data length $N = 500$ in this study), forms $N - m + 1$ vectors $X_i^m = \{u(i), u(i+1), \cdots, u(i+m-1)\}$ for $1 \le i \le N - m + 1$, where X_i^m is the vector of m data points from $u(i)$ to $u(i + m - 1)$. The distance between two such vectors X_i^m and X_j^m is defined as: $d_{i,j}^m = d\left[X_i^m, X_j^m\right] = \max_{k=0}^{m-1} |u(i+k) - u(j+k)|$. Denote by $B_i^m(r)$ the number of j that meet $d_{i,j}^m \le r$ and $A_i^m(r)$ that $d_{i,j}^{m+1} \le r$ for $1 \le j \le N-m$. The SampEn is then defined as

$$\mathrm{SampEn}(m, r, N) = -\ln\left(\sum_{i=1}^{N-m} A_i^m(r) \Big/ \sum_{i=1}^{N-m} B_i^m(r)\right) \tag{A1}$$

where embedded dimension $m = 2$, threshold $r = 0.2$ and the data length $N = 500$.

In order to better understand why it is suitable for signal quality assessment of a filtered aECG signal, McSharry's ECG model (McSharry *et al* 2003) was used to simulate both the mECG and fECG signals, which were then integrated to generate clean aECG signals. McSharry's ECG model is a dynamical model for generating ECG signals and is based on three coupled ordinary differential equations, which are listed as follows (McSharry *et al* 2003):

$$\begin{aligned} \dot{x} &= \alpha x - w y \\ \dot{y} &= \alpha y + w x \\ \dot{z} &= \sum_{i \in \{P,Q,R,S,T\}} a_i \Delta\theta_i \exp\left(-\frac{\Delta\theta_i^2}{2b_i^2}\right) - (z - z_0) \end{aligned} \tag{A2}$$

Table A1. The parameter ranges for the characteristic waves and their occurrence times of the simulated mECG.

Parameters	Characteristic waves of synthetic mECG				
	P wave	Q wave	R wave	S wave	T wave
a_i	[1.5 2.5]	[− 5 − 3]	[20 30]	[− 8 − 5]	[1 2]
b_i	[0.22 0.28]	[0.08 0.12]	[0.09 0.11]	[0.08 0.12]	[0.35 0.45]
θ_i (radians)	[-0.4π -0.3π]	[-0.1π -0.05π]	0	[0.05π 0.1π]	[0.3π 0.6π]
Occurrence time (% of RR interval)	[− 25 − 15]	[− 8 − 3]	0	[3 8]	[25 35]

where $\alpha = 1 - \sqrt{x^2 + y^2}$, w is the angular velocity of the trajectory as it moves around the limit cycle, a_i, b_i and θ_i are, respectively, amplitude, half-width and phase parameters for the P, Q, R, S and T waves of the ECG, $\Delta\theta_i = (\theta - \theta_i) \bmod 2\pi$, $\theta = \arctan(y/x)$, z_0 is the baseline wander to simulate the respiratory component, which is set to 0 in this study since the baseline wander (0 ~ 8 Hz) of the original aECG signals has been removed.

To simulate mECG, the parameters initialization are: a_i, b_i, θ_i and the occurrence time of the five sub-waves (P, Q, R, S and T) are set as random values from the specified ranges in table A1, the mean RR interval is set as a random value between the range 600 ~ 1000 ms (HR equals 60 ~ 100 beat min^{-1}). For fECG, the amplitude parameter a_i is randomly set as λ ($0.05 \leq \lambda \leq 0.4$) times the amplitude parameter a_i of mECG, the mean RR interval is set as a random value between the range 375 ~ 500 ms (HR equals 120 ~ 160 beat min^{-1}) (Pildner von Steinburg *et al* 2013), other parameter settings are the same as mECG. The negative in occurrence time means before the R wave and positive means after the R wave. For parameters a_i, b_i, θ_i, the occurrence time and RR interval in both mECG and fECG, there is beat-by-beat variability whereas the variability is limited no more than 10%.

Next, different levels of noise were added to the clean aECG signals. To simulate practical situations, four types of noise were added to the clean aECG signals: Gaussian noise, power line interference, baseline drift and non-linear noise. Power line interference used the 50 Hz sine wave and baseline drift also used a sine wave with a randomly determined frequency value below 2 Hz. Non-linear noise used the logistic sequence, which was generated by the following iteration function

$$x(n+1) = \text{w} * x(n) * (1 - x(n)) \tag{A3}$$

where the initial value $x(0)$ is in the range of 0.1 and 0.9. ω is a constant parameter that determines the complexity of the sequence and herein set as 3.9.

The SNR was used to assess the noise levels and was defined as: $\text{SNR} = 10 \times \log_{10}(P_{\text{ECG}} / P_{\text{noise}})$, where P_{ECG} denotes the power of clean aECG signal and P_{noise} denotes the power of all noises. The simulated noisy aECG signals were also pre-processed by the filtering procedure in section 2.3.1 (with notch filter, baseline removing and high frequency filtering). Figure A1(*a*) shows an example of a clean aECG waveform ($\lambda = 0.25$) as well as filter aECG signals with different SNR levels. From top to bottom, there are, respectively, the clean aECG waveform and aECG waveforms with SNR 30 dB, 25 dB, 20 dB, 15 dB, 10 dB, 5 dB and 0 dB.

One hundred repeats of these clean and filtered aECG signals at seven types of SNR levels were generated. Their mean and SD of SampEn were calculated with different r values (r = 0.10, 0.15, 0.20 and 0.25). As shown in figure A1(*b*), for each r value, SampEn stays at

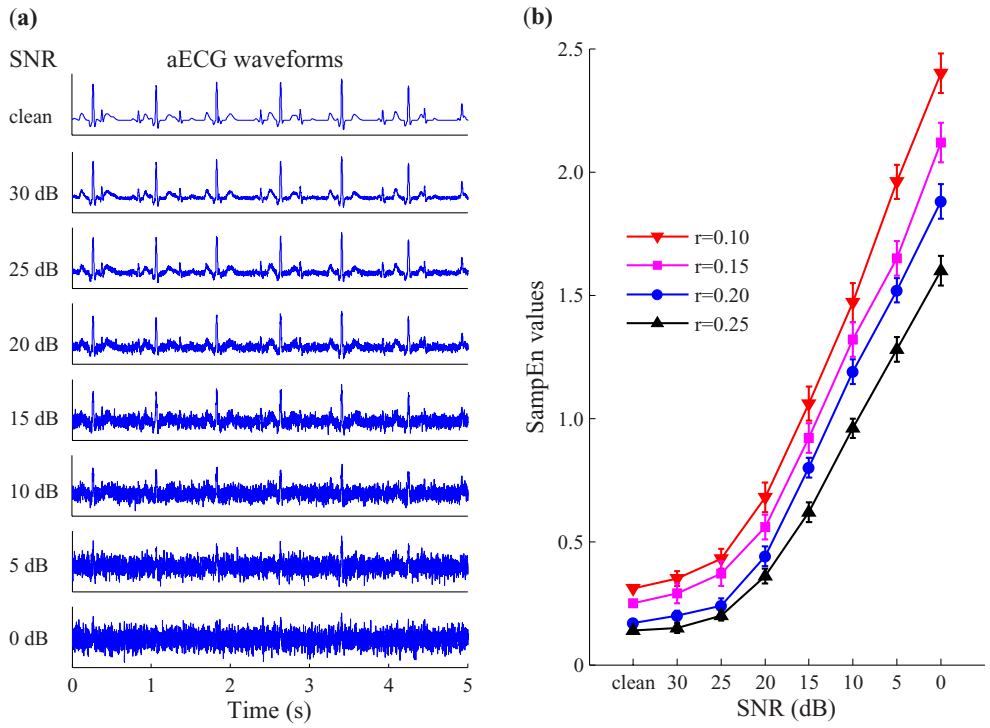

Figure A1. (*a*) Examples of simulated aECG waveforms (amplitude ratio $\lambda = 0.25$) with different SNR levels. (*b*) Mean and standard deviation (SD) of SampEn values from 100 repeats. The results with different *r* values are given.

a constant level for signals with high SNR and then rises quickly when the SNR drops. It is therefore rational to select a fixed threshold of SampEn to identify the noisy aECG signals. It also shows that the SDs of SampEn are relatively small for all SNR levels and for all four *r* values, suggesting that it is stable to use SampEn to assess the aECG signals with different noise levels.

References

Akay M and Mulder E 1996 Examining fetal heart-rate variability using matching pursuits *IEEE Eng. Med. Biol.* **15** 64–7

Andreotti F, Riedl M, Himmelsbach T, Wedekind D, Zaunseder S, Wessel N and Malberg H 2013 Maternal signal estimation by Kalman filtering and template adaptation for fetal heart rate extraction *Proc. Comput. Cardiol.* **40** 193–6

Behar J, Oster J and Clifford G D 2013 Non invasive FECG extraction from a set of abdominal sensors *Proc. Comput. Cardiol.* **40** 297–300

Camps-Valls G, Martinez-Sober M, Soria-Olivas E, Magdalena-Benedito R, Calpe-Maravilla J and Guerrero-Martinez J 2004 Foetal ECG recovery using dynamic neural networks *Artif. Intell. Med.* **31** 197–209

Clifford G D, Sameni R, Ward J, Robinson J and Wolfberg A J 2011 Clinically accurate fetal ECG parameters acquired from maternal abdominal sensors *Am. J. Obstet. Gynecol.* **205** e1–5

Clifford G D, Silva I, Behar J and Moody G 2014 Noninvasive fetal ECG analysis *Physiol. Meas.* **35** 1521

De Lathauwer L, De Moor B and Vandewalle J 2000 Fetal electrocardiogram extraction by blind source subspace separation *IEEE Trans. Biomed. Eng.* **47** 567–72

Di Marco L Y, Marzo A and Frangi A 2013 Multichannel foetal heartbeat detection by combining source cancellation with expectation-weighted estimation of fiducial points *Proc. Comput. Cardiol*. **40** 329–32

Di Maria C, Duan W F, Bojarnejad M, Pan F, King S, Zheng D C, Murray A and Langley P 2013 An algorithm for the analysis of foetal ECGs from 4-channel non-invasive abdominal recordings *Proc. Comput. Cardiol*. **40** 305–8

Hamilton P S 1996 A comparison of adaptive and nonadaptive filters for reduction of power line interference in the ECG *IEEE Trans. Biomed. Eng*. **43** 105–9

Hasan M A, Reaz M B, Ibrahimy M I, Hussain M S and Uddin J 2009 Detection and processing techniques of FECG signal for fetal monitoring *Biol. Proced. Online* **11** 263–95

Ingemarsson I 2009 Fetal monitoring during labor *Neonatology* **95** 342–6

Jolliffe I 2005 Principal component analysis *Encyclopedia of Statistics in Behavioral Science* (Hoboken, NJ: Wiley)

Kanjilal P P, Palit S and Saha G 1997 Fetal ECG extraction from single-channel maternal ECG using singular value decomposition *IEEE Trans. Biomed. Eng*. **44** 51–9

Kennedy R G 1998 Electronic fetal heart rate monitoring: retrospective reflections on a twentieth-century technology *J. R. Soc. Med*. **91** 244–50

Khamene A and Negahdaripour S 2000 A new method for the extraction of fetal ECG from the composite abdominal signal *IEEE Trans. Biomed. Eng*. **47** 507–16

Lai K C and Shynk J J 2002 A successive cancellation algorithm for fetal heart-rate estimation using an intrauterine ECG signal *IEEE Trans. Biomed. Eng*. **49** 943–54

Li Q, Mark R G and Clifford G D 2008 Robust heart rate estimation from multiple asynchronous noisy sources using signal quality indices and a Kalman filter *Physiol. Meas.* **29** 15–32

Lipponen J A and Tarvainen M P 2013 Advanced maternal ECG removal and noise reduction for application of fetal QRS detection *Proc. Comput. Cardiol*. **40** 161–4

Liu C Y and Li P 2013 Systematic methods for fetal electrocardiographic analysis: Determining the fetal heart rate, RR interval and QT interval *Proc. Comput. Cardiol*. **40** 309–12

Liu C Y, Li K, Zhao L N, Liu F, Zheng D C, Liu C C and Liu S T 2013 Analysis of heart rate variability using fuzzy measure entropy *Comput. Biol. Med*. **43** 100–8

Liu C Y, Li L P, Zhao L N, Zheng D C, Li P and Liu C C 2012 A combination method of improved impulse rejection filter and template matching for identification of anomalous intervals in electrocardiographic RR sequences *J. Med. Biol. Eng*. **32** 245–50

Liu C Y, Li P, Zhao L N, Liu F F and Wang R X 2011a Real-time signal quality assessment for ECGs collected using mobile phones *Proc. Comput. Cardiol*. **38** 357–60

Liu C Y, Liu C C, Shao P, Li L P, Sun X, Wang X P and Liu F 2011b Comparison of different threshold values r for approximate entropy: application to investigate the heart rate variability between heart failure and healthy control groups *Physiol. Meas*. **32** 167–80

Martens S M M, Rabotti C, Mischi M and Sluijter R J 2007 A robust fetal ECG detection method for abdominal recordings *Physiol. Meas*. **28** 373–88

McSharry P E, Clifford G D, Tarassenko L and Smith L A 2003 A dynamical model for generating synthetic electrocardiogram signals *IEEE Trans. Biomed. Eng*. **50** 289–94

Najafabadi F S, Zahedi E and Mohd Ali M A 2006 Fetal heart rate monitoring based on independent component analysis *Comput. Biol. Med*. **36** 241–52

Outram N J, Ifeachor E C, Van Eetvelt P W J and Curnow J S H 1995 Techniques for optimal enhancement and feature extraction of fetal electrocardiogram *IEEE Proc. Sci. Meas. Technol.* **142** 482–9

Pan J and Tompkins W J 1985 A real-time QRS detection algorithm *IEEE Trans. Biomed. Eng*. **32** 230–6

Park Y C, Lee K Y, Youn D H, Kim N H, Kim W K and Park S H 1992 On detecting the presence of fetal R-wave using the moving averaged magnitude difference algorithm *IEEE Trans. Biomed. Eng*. **39** 868–71

Pildner von Steinburg S, Boulesteix A L, Lederer C, Grunow S, Schiermeier S, Hatzmann W, Schneider K T and Daumer M 2013 What is the 'normal' fetal heart rate? *PeerJ* **1** e82

Podziemski P and Gierałtowski J 2013 Fetal heart rate discovery: algorithm for detection of fetal heart rate from noisy, noninvasive fetal ECG recordings *Proc. Comput. Cardiol*. **40** 333–6

Quan P, Zhang D, Guanzhong D and Hongcai Z 1999 Two denoising methods by wavelet transform *IEEE Trans. Signal Proces*. **47** 3401–6

Richman J S and Moorman J R 2000 Physiological time-series analysis using approximate entropy and sample entropy *Am. J. Physiol. Heart Circ. Physiol*. **278** H2039–49

Richter M, Schreiber T and Kaplan D T 1998 Fetal ECG extraction with nonlinear state-space projections *IEEE Trans. Biomed. Eng*. **45** 133–7

Rodrigues R 2013 Fetal ECG detection in abdominal recordings: a method for QRS location *Proc. Comput. Cardiol*. **40** 325–8

Sameni R and Clifford G D 2010 A review of fetal ECG signal processing; issues and promising directions *Open Pacing Electrophysiol. Ther. J*. **3** 4–20

Sameni R, Shamsollahi M B and Jutten C 2008 Model-based Bayesian filtering of cardiac contaminants from biomedical recordings *Physiol. Meas*. **29** 595–613

Silva I, Behar J, Zhu T T, Oster J, Clifford G D and Moody G B 2013 Noninvasive fetal ECG: the PhysioNet/Computing in Cardiology challenge 2013 *Proc. Comput. Cardiol*. **40** 149–52

Varanini M, Tartarisco G, Billeci L, Macerata A, Pioggia G and Balocchi R 2013 A multi-step approach for non-invasive fetal ECG analysis *Proc. Comput. Cardiol*. **40** 281–4